ACS NANO

Large-Scale Synthesis, Crystal Structure, and Optical Properties of the $Ag_{146}Br_2(SR)_{80}$ Nanocluster

Yongbo Song,[†,‡] Kelly Lambright,[§] Meng Zhou,[‡] Kristin Kirschbaum,[§] Ji Xiang,[†] Andong Xia,[∥] Manzhou Zhu,[*,†] and Rongchao Jin[*,‡]

[†]Department of Chemistry and Center for Atomic Engineering of Advanced Materials, Anhui University, Hefei, Anhui 230601, China

[‡]Department of Chemistry, Carnegie Mellon University, Pittsburgh, Pennsylvania 15213, United States

[§]Department of Chemistry and Biochemistry, University of Toledo, Toledo, Ohio 43606, United States

[∥]Beijing National Laboratory for Molecular Sciences (BNLMS), Key Laboratory of Photochemistry, Institute of Chemistry, Chinese Academy of Sciences, Beijing 100190, China

DOI: 10.1021/acsnano.8b04233

Received: June 4, 2018
Accepted: August 16, 2018
Published: August 16, 2018

ARIJIT

06/10/2018

RELEVANT TO THE GROUP :

The Super stable 25 kDa Monolayer Protected Silver Nanoparticle: Measurements and Interpretation as an Icosahedral $Ag_{152}(SCH_2CH_2Ph)_{60}$ Cluster.

dx.doi.org/10.1021/nl303220x | Nano Lett. 2012, 12, 5861−5866

NANO LETTERS

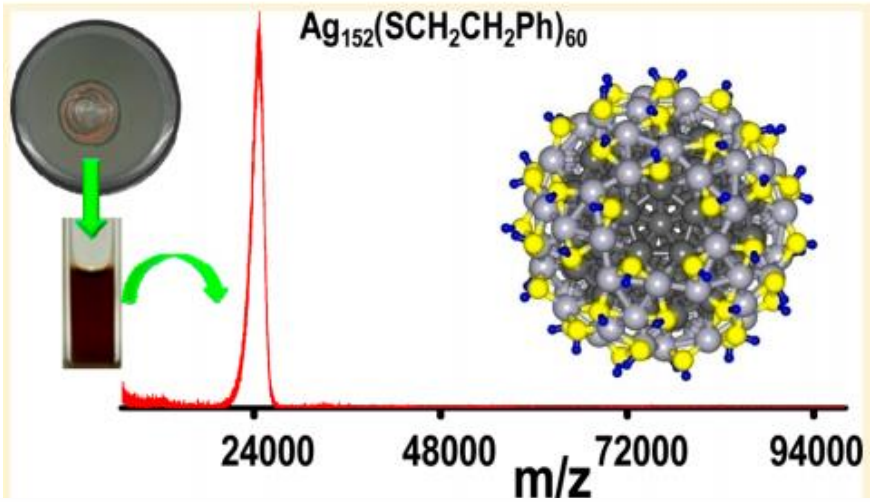

JACS
JOURNAL OF THE AMERICAN CHEMICAL SOCIETY
Communication
Cite This: J. Am. Chem. Soc. 2018, 140, 5691−5695
pubs.acs.org/JACS

Sharp Transition from Nonmetallic Au_{246} to Metallic Au_{279} with Nascent Surface Plasmon Resonance

Tatsuya Higaki,[†,#] Meng Zhou,[†,#] Kelly J. Lambright,[‡] Kristin Kirschbaum,[‡] Matthew Y. Sfeir,[§] and Rongchao Jin*[,†]

[†]Department of Chemistry, Carnegie Mellon University, Pittsburgh, Pennsylvania 15213, United States
[‡]Department of Chemistry and Biochemistry, University of Toledo, Toledo, Ohio 43606, United States
[§]Center for Functional Nanomaterials, Brookhaven National Laboratory, Upton, New York 11973, United States

IN THIS PAPER.....

- A stable silver nanocluster $Ag_{146}Br_2(SR)_{80}$ (where SR = 4 isopropylbenzene thiolate)- with its structure solved by X ray crystallography.
- Gram scale synthesis with high yield is achieved by a one pot synthesis, which offers opportunities for functionalization and applications.
- This silver nanocluster possesses a core–shell structure with a Ag_{51} core surrounded by a shell of $Ag_{95}Br_2S_{80}$. The Ag_{51} core can be viewed as a distorted decahedron, endowing this nanocluster with quantized electronic transitions.
- Temperature-dependent optical absorption and ultrafast electron dynamics are conducted to explore the relationship between the properties and structure, demonstrating that the distorted metal core and “flying saucer”-like shape of this nanocluster have significant effects on the electronic behavior.
- A comparison with multiple sizes of Ag nanoclusters also provides some insights into the evolution from molecular to metallic behavior.

Synthesis of Ag_{146} nanocluster :

Aqueous $AgNO_3$ (DCM Solution) + 4-isopropylbenzenethiol + TPPB

↓

Ag- thiolate (Ag-SR) complex (Yellow Precipitate)

↓ **Aqueous $NaBH_4$ reduction**

Blackish silver nanocluster

↓ **Diffusion of Acetone in DCM solution**

Dark crystal

Typical **10-fold** **20-fold** **100-fold**

Figure S8. Photographs of the reactions performed at different scales.

Crystal Structure for $Ag_{146}Br_2(SR)_{80}$

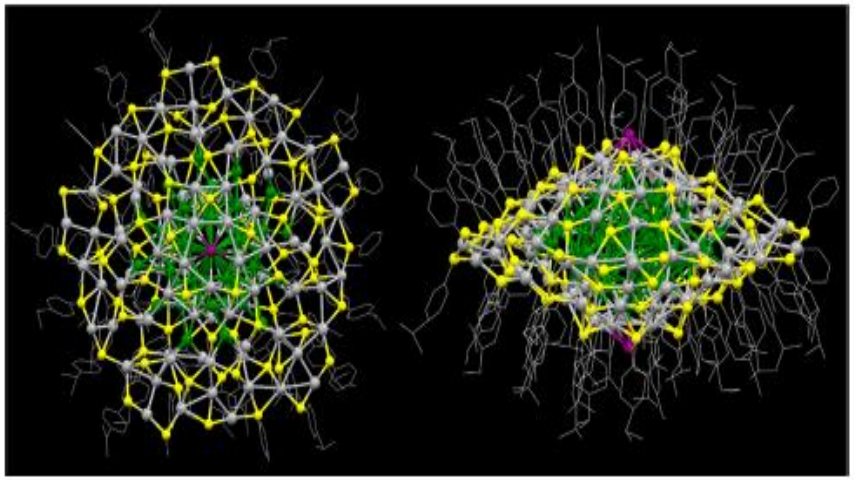

Figure 1. Top (left) and side (right) views of the total structure of the $Ag_{146}Br_2(TIBT)_{80}$ nanocluster. Color labels: dark gray/green = Ag, yellow = S, purple = Br; the carbon tails are shown in wire-frame mode.

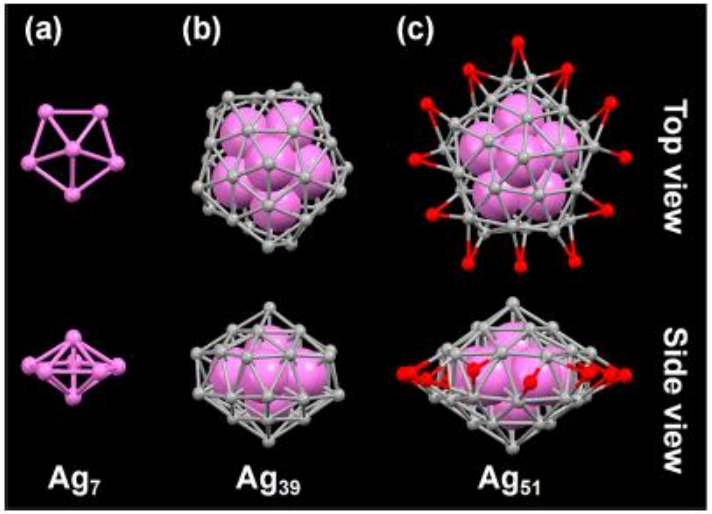

Figure 2. Top and side views of the three shells in the Ag_{51} kernel of the $Ag_{146}Br_2(TIBT)_{80}$ nanocluster: (a) the decahedral seven-atom shell (magenta); (b) the 32-atom shell (gray); (c) the ring-shaped 12-atom (red).

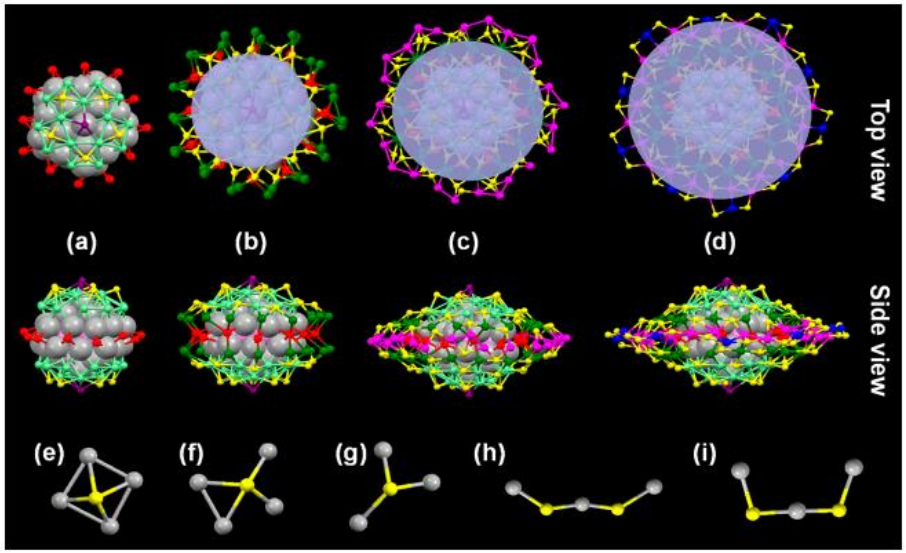

Figure 3. Top and side view of the four shells in the $Ag_{95}S_{80}Br_2$ surface of the Ag_{146} nanocluster: (a) the first $Ag_{30}S_{10}Br_2$ part (light blue); (b) the second $Ag_{30}S_{20}$ part (green); (c) the third $Ag_{25}S_{30}$ part (magenta); (d) the fourth $Ag_{10}S_{20}$ part (blue); (e–i) the different types of S–Ag motifs observed on the surface of the Ag_{146} nanocluster.

ESI MS DATA ANALYSIS :

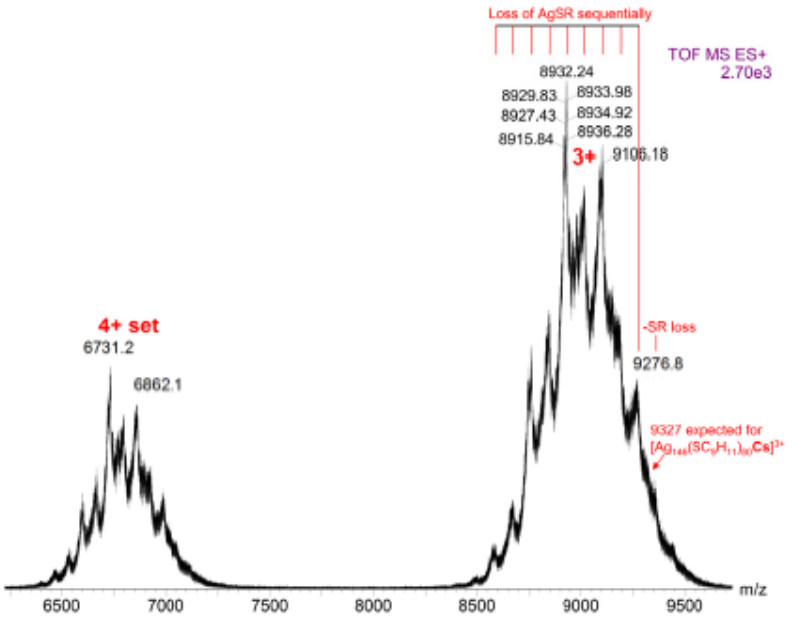

Figure S6. ESI mass spectrum of the silver nanocluster (positive mode). Note: Sequential losses of ligand (-SR) and/or Ag-SR fragment occurred in the analysis.

Table S1. Analysis of the ESI mass spectral peaks for the silver nanocluster.

$[Ag_{146}(SC_9h_{11})_{79}Cs]^{3+}$	9276.8	$[Ag_{145}(SC_9h_{11})_{78}Cs]^{3+}$	9189.5	$[Ag_{144}(SC_9h_{11})_{77}Cs]^{3+}$	9104.4
$[Ag_{143}(SC_9h_{11})_{76}Cs]^{3+}$	9017.1	$[Ag_{142}(SC_9h_{11})_{75}Cs]^{3+}$	8932.2	$[Ag_{141}(SC_9h_{11})_{74}Cs]^{3+}$	8854.6
$[Ag_{140}(SC_9h_{11})_{73}Cs]^{3+}$	8759.1	$[Ag_{139}(SC_9h_{11})_{72}Cs]^{3+}$	8672.2	$[Ag_{138}(SC_9h_{11})_{71}Cs]^{3+}$	8585.7
$[Ag_{146}(SC_9h_{11})_{79}Cs_2]^{4+}$	6990.6	$[Ag_{145}(SC_9h_{11})_{78}Cs_2]^{4+}$	6924.9	$[Ag_{144}(SC_9h_{11})_{77}Cs_2]^{4+}$	6862.1
$[Ag_{143}(SC_9h_{11})_{76}Cs_2]^{4+}$	6795.8	$[Ag_{142}(SC_9h_{11})_{75}Cs_2]^{4+}$	6731.2	$[Ag_{141}(SC_9h_{11})_{74}Cs_2]^{4+}$	6666.3
$[Ag_{140}(SC_9h_{11})_{73}Cs_2]^{4+}$	6601.7	$[Ag_{139}(SC_9h_{11})_{72}Cs_2]^{4+}$	6536.9	$[Ag_{138}(SC_9h_{11})_{71}Cs_2]^{4+}$	6472.2

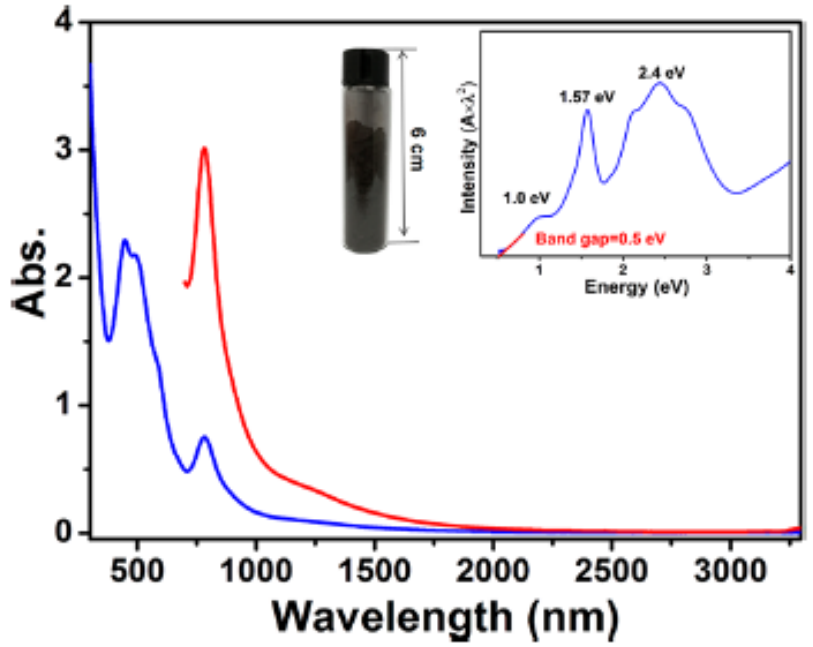
Abs.
Wavelength (nm)
6 cm
Intensity (A×λ²)
1.57 eV
2.4 eV
1.0 eV
Band gap=0.5 eV
Energy (eV)

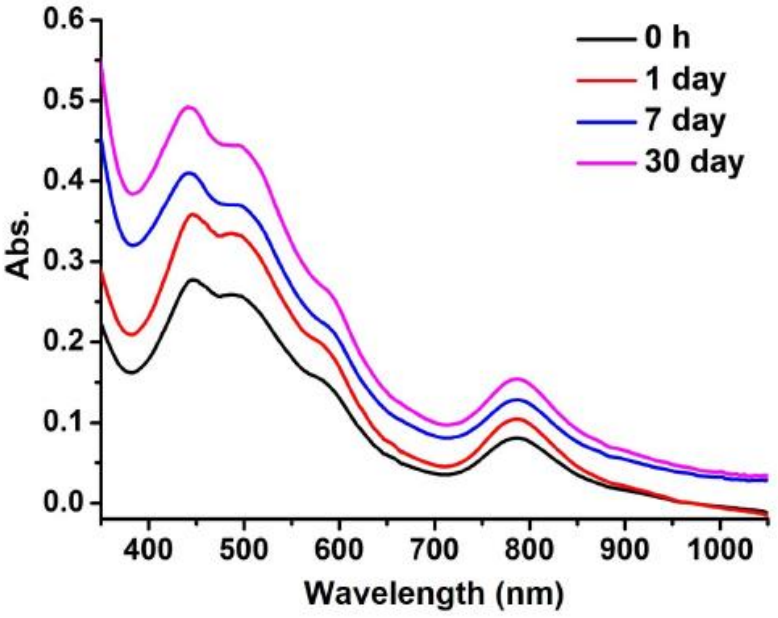
0 h
1 day
7 day
30 day
Abs.
Wavelength (nm)

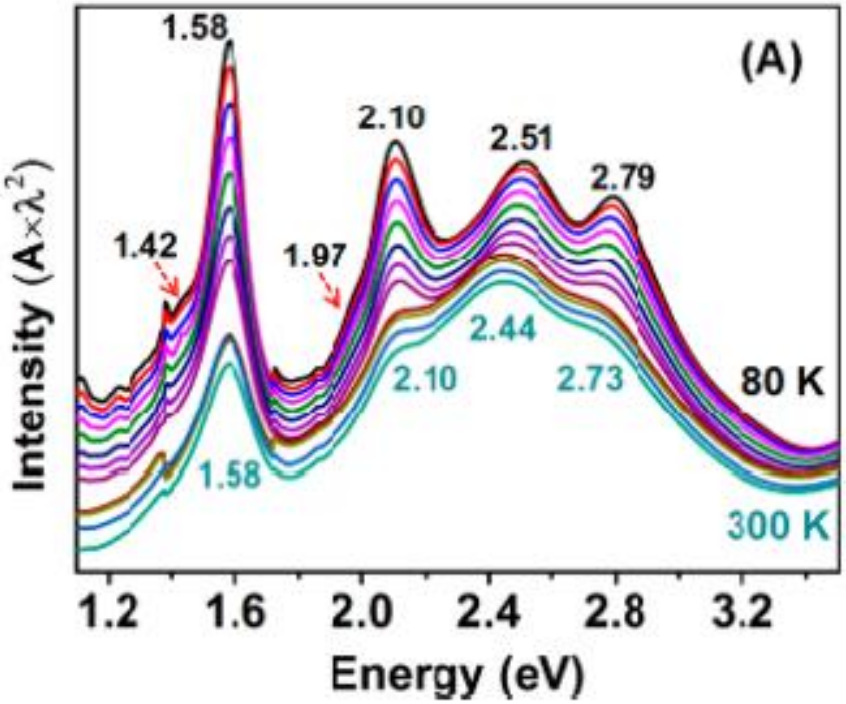
(A)
1.58
2.10
2.51
2.79
1.42
1.97
2.44
2.10
2.73
80 K
1.58
300 K
Intensity (A×λ²)
Energy (eV)

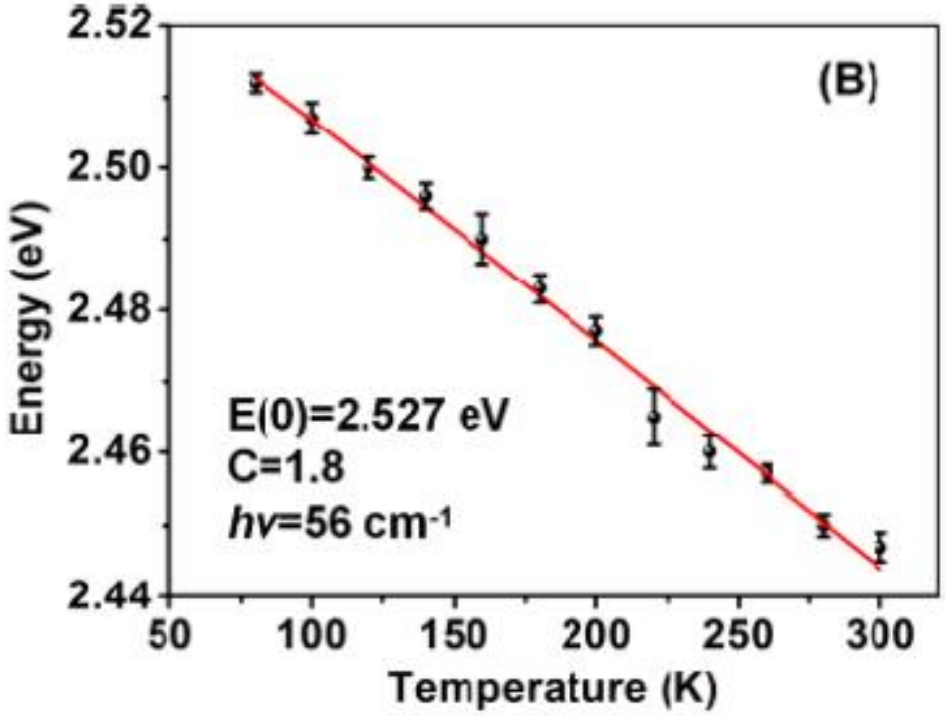
(B)
E(0)=2.527 eV
C=1.8
hν=56 cm⁻¹
Energy (eV)
Temperature (K)

O’Donnell Chen equation relates the energy (E(T)) to temperature by the following expression :

$$E(T) = E(0) - \langle C \rangle \langle h\nu \rangle \left[\coth\left(\frac{\langle h\nu \rangle}{2kT} \right) - 1 \right]$$

where E(0) is the absorption position at 0 K, C is the electron-phonon coupling constant, and hv is the average phonon mode which contributes to the electron−phonon interaction. From the fitting, the average phonon frequency is determined to be 7.2 meV (56 cm^{-1}).

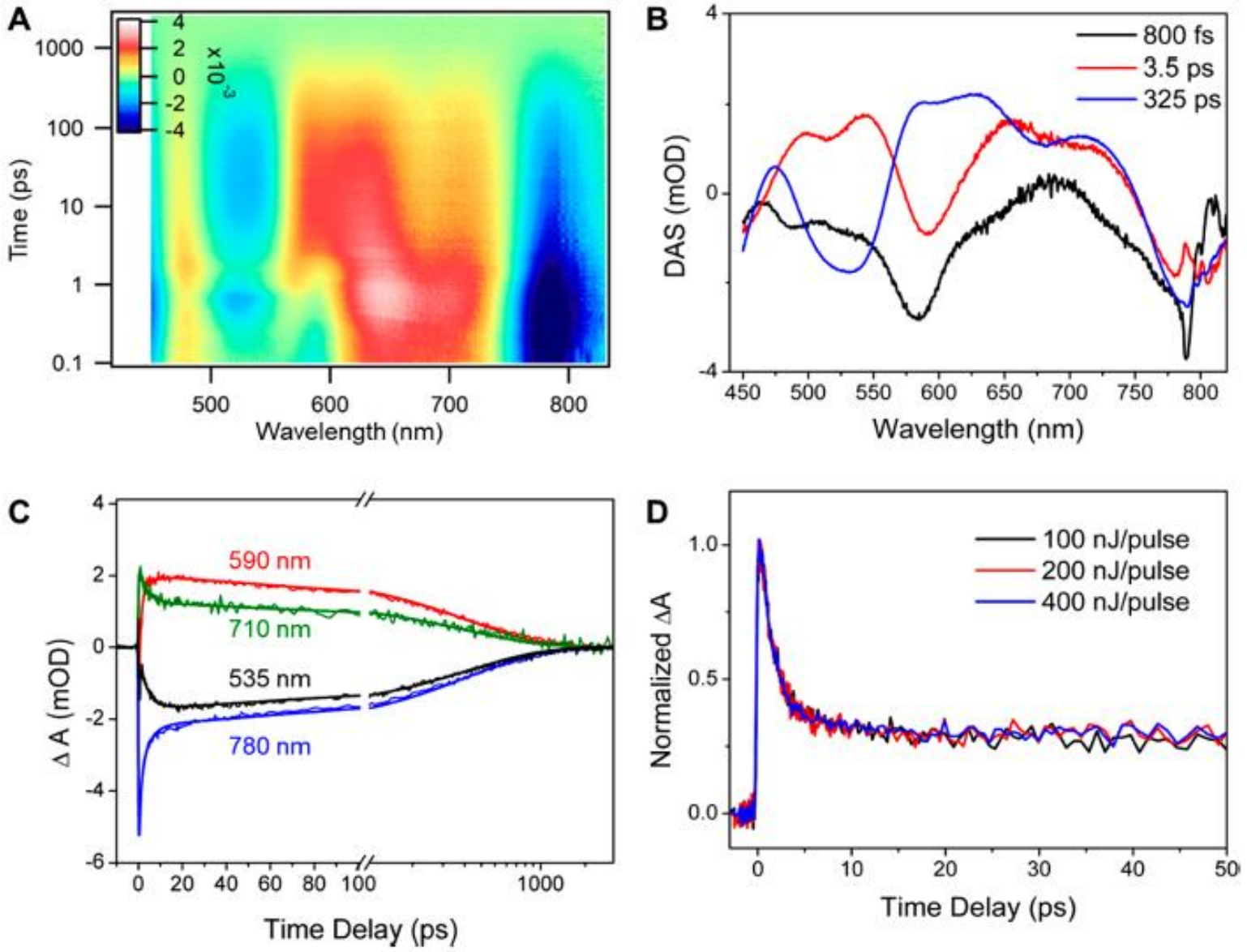

Figure 6. Ultrafast transient absorption spectroscopy characterization of the Ag146 nanocluster. (A) Transient absorption data map pumped at 430 nm. (B) Decay-associated spectra (DAS) obtained from global fitting. (C) Kinetic traces at selected wavelengths and the corresponding fits. (D) Kinetic traces probed at the GSB around 780 nm at different pump fluences.

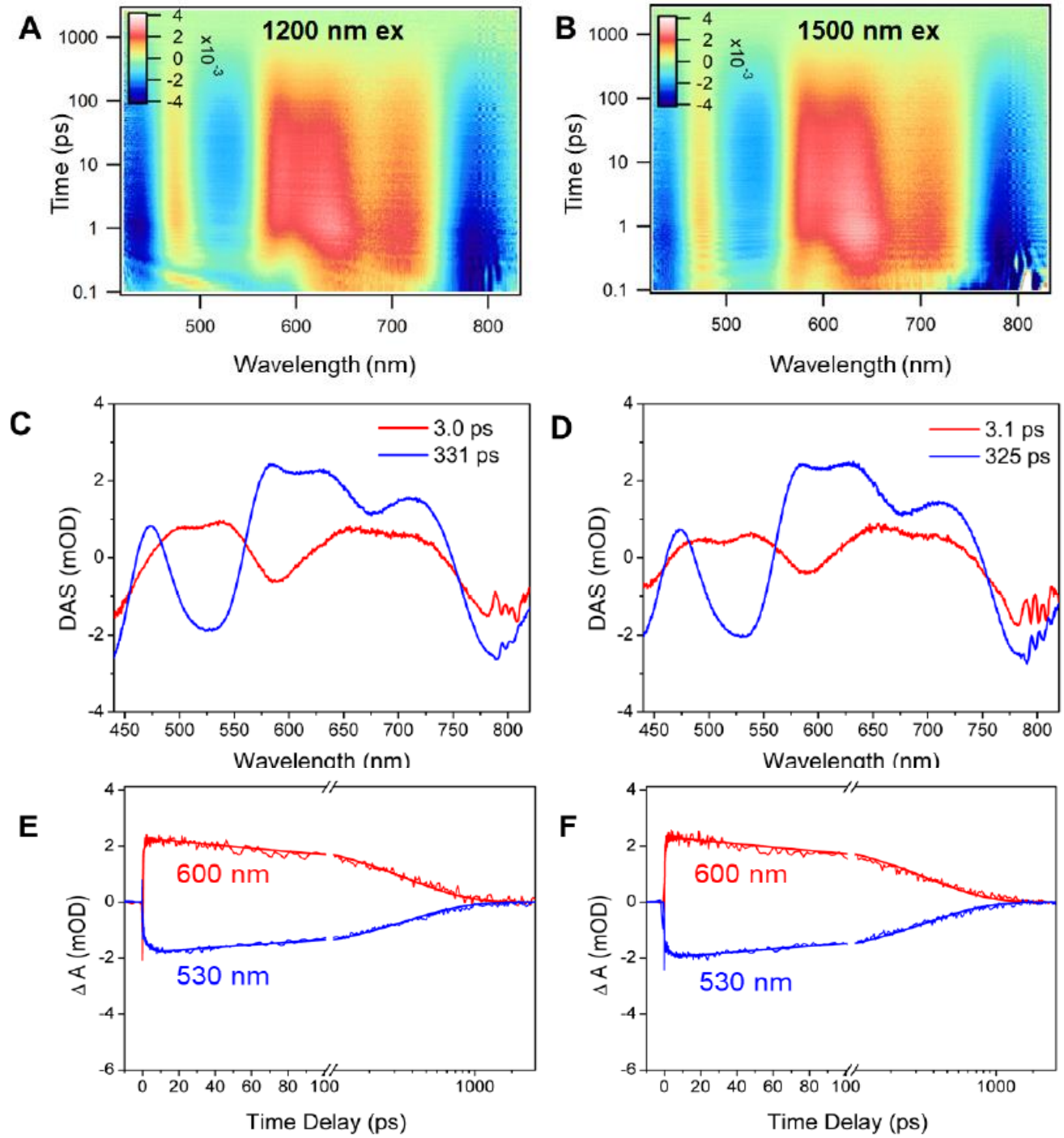

Figure S9. Ultrafast transient absorption spectroscopic analysis of the silver nanocluster: (A-B) Transient absorption data map pumped at 1200 nm and 1500 nm, respectively; (C-D) Decay associated spectra (DAS) obtained from global fitting; (E-F) Kinetic traces and fitting at selected wavelengths. Note: A, C and E are for the case of 1200 nm excitation, whereas B, D, and F for 1500 nm excitation.

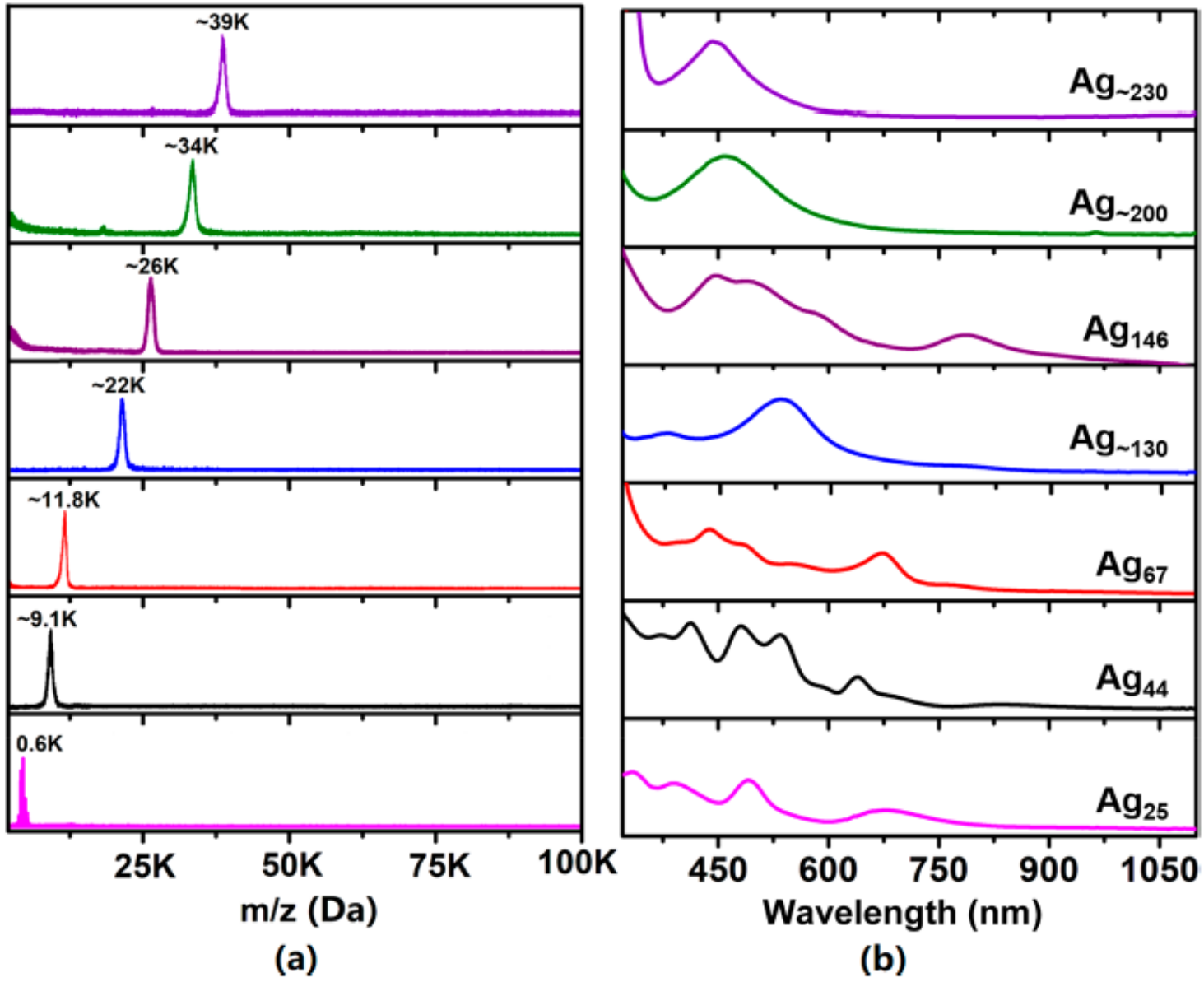

Figure 7. Different-sized silver nanoparticles spanning the molecular and metallic states. (a) Matrix-assisted laser desorption/ionization mass spectra. (b) Steady state ultraviolet−visible absorption spectra.

CONCLUSION :

- Successful synthesis of large silver nanocluster [$Ag_{146}Br_2(TIBT)_{80}$] by direct reduction of Ag(I)-SR complex with NaBH4 and gram scale synthesis is achieved for this nanocluster.
- X–ray crystallography reveals that the framework of Ag_{146} contains of decahedral Ag_{51} core, which is protected by $Ag_{95}Br_2S_{80}$ surface.
- This nanocluster exhibits an observable optical band gap and power independent electron dynamics, which indicate the molecular like nature of the nanocluster, as opposed to metallic or plasmonic.
- The successful structure determination and the molecular like optical properties of Ag146 will be a basis for future work on large-sized nanocluster.